

The intermodulation coefficient of an inhomogeneous superconductor

Kwangmoo Kim and David Stroud^{a)}

Department of Physics, The Ohio State University, Columbus, Ohio 43210

(Received 23 March 2006; accepted 27 September 2006; published online 11 December 2006)

The high- T_c cuprate superconductors are now believed to be intrinsically inhomogeneous. We develop a theory to describe how this inhomogeneity affects the intermodulation coefficient of such a material. We show that the continuum equations describing intermodulation in a superconducting layer with spatially varying properties are formally equivalent to those describing an inhomogeneous dielectric with a nonzero cubic nonlinearity. Using this formal analogy, we calculate the effect of inhomogeneity on the intermodulation coefficient in a high- T_c material, using several assumptions about the topology of the layer and some simple analytical approximations to treat the nonlinearity. For some topologies, we find that the intermodulation critical supercurrent density J_{IMD} is actually *enhanced* compared to a homogeneous medium, thereby possibly leading to more desirable material properties. We discuss this result in light of recent spatial mappings of the superconducting energy gap in BSCCO-2212. © 2006 American Institute of Physics.

[DOI: 10.1063/1.2372729]

I. INTRODUCTION

Ever since the discovery of high- T_c superconductors,¹ many workers have attempted to develop practical applications for them. One potential electronic application is as a microstrip resonator. Such a device has been developed by Willemsen *et al.*,² using a high- T_c cuprate material. Even though these devices do not work at very high current densities, they are subject to strong nonlinear effects which mix together microwaves of different frequencies. This mixing, known as intermodulation, was studied experimentally and theoretically by Willemsen *et al.*;² theoretical models to explain their measurements were developed by Dahm and Scalapino.^{3,4}

In the model of Refs. 3 and 4, the intermodulation is described in terms of an intermodulation current density J_{IMD} , which depends on both temperature and the angle between the direction of current flow and the crystal axes. An equivalent quantity was also considered by Yip and Sauls⁵ for a d -wave superconductor. Because of low-lying quasiparticles, they found that J_{IMD} was much smaller than for a corresponding s -wave superconductor and also that it depended on the angle between the in-plane current density and the \mathbf{k} vector of the gap nodes. Several other workers have also studied this intermodulation and the harmonic generation due to nonlinear effects.⁶⁻⁸

In all this work, the high- T_c cuprate superconductor was assumed to be *homogeneous*, that is, the CuO_2 layer properties were assumed independent of position within the layer. However, recent experimental work has invalidated this picture. Specifically, in optimally oxygen-doped,^{9,10} underdoped,¹¹ and slightly overdoped¹² $\text{Bi}_2\text{Sr}_2\text{CaCu}_2\text{O}_{8+\delta}$ (usually called BSCCO-2212), the superconducting energy gap was found to be *spatially varying*. This result was obtained from scanning tunneling microscopy/spectroscopy (STM/S) images of the superconducting layers. The differen-

tial tunneling conductance spectra of the sample were measured and the position-dependent gap Δ was inferred from measurements of the energy difference between two coherence peaks in the spectra above and below the Fermi level. In the underdoped sample, the gap was found to map into two distinct regions. One (called the α domains) had a gap $\Delta < 50$ meV; the other (denoted the β domains) had $\Delta > 50$ meV. The α domains were identified as superconducting, because they showed coherence peaks in the tunneling spectra. The β regions were found to be nonsuperconducting, and were identified as a pseudogap phase,^{11,12} with a large gap. It was concluded that the spatially varying superconducting energy gaps do not arise from impurities, but are instead intrinsic properties of the material. Thus, underdoped BSCCO-2212 is an intrinsically granular superconductor. Very recently, a model has been introduced to reproduce the experimental gap distribution, using the low order moments of the local density of states.¹³

In this paper, we consider how this inhomogeneity affects the intermodulation in a high- T_c superconductor, such as BSCCO-2212. As implied above, this intermodulation coefficient is actually a nonlinear transport coefficient. In fact, this coefficient describes the current dependence of the superfluid density in the superconductor. This current dependence is particularly strong in the d -wave high- T_c materials, because quasiparticles are excited even at very low applied currents. We will show that J_{IMD} is formally analogous to another coefficient, well known in the study of nonlinear dielectrics. Using this connection, we will demonstrate that J_{IMD} is very sensitive to the detailed geometry of the superconducting inhomogeneity.

We will consider only two-dimensional (2D) systems and only very low frequencies. This regime is appropriate to the cuprate superconductors, where superconductivity is believed to occur within CuO_2 planes. Our low-frequency approach should be applicable so long as the length scale of the

^{a)}Electronic mail: stroud@mps.ohio-state.edu

inhomogeneity is much smaller than the wavelength of the applied microwave fields, a condition easily satisfied at microwave frequencies.

The remainder of this paper is organized as follows. In Sec. II, we present the formalism for calculating the enhancement of J_{IMD} in an inhomogeneous 2D superconductor. In Sec. III, we give several analytical results for the relevant enhancements and for J_{IMD} , based on the analogy to a nonlinear dielectric composite. Section IV presents a concluding discussion.

II. FORMALISM

A. Intermodulation coefficients from Ginzburg-Landau theory

We begin by expressing J_{IMD} in terms of coefficients of the Ginzburg-Landau free energy density F . In the absence of a vector potential \mathbf{A} , F takes the standard form

$$F = a|\psi|^2 + \frac{b}{2}|\psi|^4 + C|\nabla\psi|^2, \quad (1)$$

where a , b , and C are appropriate constants and ψ is the complex position-dependent Ginzburg-Landau wave function. For the present problem, we will eventually assume that all three constants are functions of position. We also write $C = \hbar^2/(2m^*)$, where m^* is a quantity with dimensions of mass.

The local supercurrent density takes the usual quantum-mechanical form

$$\mathbf{J} = \frac{e^*}{2m^*}[\psi^*(-i\hbar\nabla)\psi + \text{c.c.}], \quad (2)$$

where e^* is the charge of a Cooper pair and ‘‘c.c.’’ denotes a complex conjugate. We write $\psi = |\psi|\exp(i\phi)$ and initially assume that ϕ , but not $|\psi|$, is position dependent, so that

$$\mathbf{J} = \frac{e^*}{m^*}|\psi|^2(\hbar\nabla\phi). \quad (3)$$

In the limit of very small current density, the wave function is found by minimizing the free energy with respect to $|\psi|^2$, which gives the standard expression $|\psi|^2 = -a/b$. This quantity is positive if $a < 0$.

If there is a finite phase gradient, F takes the form

$$F = a|\psi|^2 + \frac{b}{2}|\psi|^4 + \frac{\hbar^2}{2m^*}|\psi|^2|\nabla\phi|^2. \quad (4)$$

Minimizing with respect to the modulus of the wave function at fixed $\nabla\phi$, we find that

$$|\psi|^2 = -\frac{[a + (\hbar^2/(2m^*))|\nabla\phi|^2]}{b}. \quad (5)$$

The corresponding current density takes the form

$$\mathbf{J} = -\frac{e^*}{m^*}\left[\frac{a}{b}(\hbar\nabla\phi) + \frac{\hbar^2}{2m^*b}|\nabla\phi|^2\hbar\nabla\phi\right]. \quad (6)$$

In the above discussion, we have assumed that $|\psi|$ is position independent, so that $\nabla|\psi| = 0$. Even if $\nabla|\psi| \neq 0$, Eq. (3) for \mathbf{J} remains valid. However, there is an extra term in the

free energy density; so Eq. (5) and hence Eq. (6) do not hold exactly. Nevertheless, we shall assume that the most important effects of inhomogeneity can be included by writing

$$\mathbf{J} = K_1(\mathbf{x})\nabla\phi(1 - K_2(\mathbf{x})|\nabla\phi|^2), \quad (7)$$

with appropriate coefficients $K_1(\mathbf{x})$ and $K_2(\mathbf{x})$.

We now show that Eq. (6) (for a uniform superconductor) contains the intermodulation phenomenon of interest. First, we rewrite Eq. (6) for a uniform superconductor as

$$\mathbf{J} = K_1\nabla\phi(1 - K_2|\nabla\phi|^2), \quad (8)$$

where K_1 and K_2 are related to the original a , b , and m^* . If $\mathbf{A} \neq 0$, in order for the gradient to remain gauge invariant, we must make the replacement $-i\hbar\nabla \rightarrow -i\hbar\nabla - (e^*/c)\mathbf{A}$, or equivalently

$$\nabla\phi \rightarrow \nabla\phi - \frac{e^*}{\hbar c}\mathbf{A}. \quad (9)$$

Thus, if $\mathbf{A} \neq 0$ but the phase is uniform, we must rewrite Eq. (8) as

$$\mathbf{J} = -\frac{e^*K_1}{\hbar c}\mathbf{A}\left[1 - \frac{e^{*2}K_2}{\hbar^2c^2}|\mathbf{A}|^2\right]. \quad (10)$$

To order A^3 (or J^3), we can replace $|\mathbf{A}|^2$ on the right-hand side of this expression by $[\hbar c/(e^*K_1)]^2|\mathbf{J}|^2$, which gives

$$\mathbf{J} = -\frac{e^*K_1}{\hbar c}\mathbf{A}\left[1 - \frac{J^2}{J_{\text{IMD}}^2}\right], \quad (11)$$

where

$$J_{\text{IMD}}^2 = \frac{K_1^2}{K_2}. \quad (12)$$

Finally, we show that Eq. (11) implies a current-dependent penetration depth. To see this, we first take the curl of Eq. (11) in the low current limit to get

$$\nabla \times \mathbf{J} = -\alpha'\mathbf{B}, \quad (13)$$

where $\alpha' = e^*K_1/(\hbar c)$. When this equation is combined with Ampere's law, $\nabla \times \mathbf{B} = 4\pi\mathbf{J}/c$, we get $\nabla^2\mathbf{J} - [1/\lambda^2(T,0)]\mathbf{J} = 0$, where

$$\frac{1}{\lambda^2(T,0)} = \frac{4\pi e^*K_1}{\hbar c^2}, \quad (14)$$

and $\lambda(T,0)$ is the zero-current penetration depth at temperature T . Thus finally

$$\mathbf{J} = -\frac{c}{4\pi\lambda^2(T,0)}\mathbf{A}\left[1 - \frac{J^2}{J_{\text{IMD}}^2}\right]. \quad (15)$$

Equation (15) has the form $\mathbf{J} = -\mu(T,J)\mathbf{A}$, where $\mu(T,J) = c/[4\pi\lambda^2(T,J)]$, $\lambda(T,J)$ being the temperature- and current-dependent penetration depth. Thus, Eq. (15) is equivalent to

$$\frac{1}{\lambda^2(T,J)} = \frac{1}{\lambda^2(T,0)}\left[1 - \frac{J^2}{J_{\text{IMD}}^2}\right]. \quad (16)$$

To order J^2 , this result is equivalent to Eq. (7) of Ref. 3.¹⁴

B. Estimate of Ginzburg-Landau parameters for cuprate superconductors

Within the Ginzburg-Landau formalism, the penetration depth is related to the order parameter $|\psi|$ by

$$\frac{1}{\lambda(T,0)} = \left[\frac{4\pi e^*{}^2 |\psi|^2}{m^* c^2} \right]^{1/2}, \quad (17)$$

and $|\psi|^2 = -a/b$, provided that $a < 0$. Taking $a = -\alpha(1 - T/T_{c0})$, where $\alpha > 0$ and T_{c0} is the mean-field transition temperature, we obtain

$$|\psi|^2 = \alpha(1 - T/T_{c0})/b \quad (18)$$

and

$$\frac{1}{\lambda^2(T,0)} = \frac{4\pi e^*{}^2 \alpha(1 - T/T_{c0})}{m^* c^2 b}. \quad (19)$$

In Eq. (19), ψ which has dimensions of a wave function. Lacking an accepted microscopic theory for the high- T_c cuprates, we may estimate α and b using BCS theory, as discussed, for example, by de Gennes.¹⁵ The result is

$$\alpha = \frac{\hbar^2}{2m^* \xi_0^2} \quad (20)$$

and

$$b = \frac{\hbar^4}{4m^*{}^2 \xi_0^4 N(0)(k_B T_{c0})^2}. \quad (21)$$

Here, $N(0)$ is the single-particle density of states at the Fermi energy (measured in states per unit energy per unit volume) and ξ_0 is a temperature-independent coherence length. The penetration depth is then found to be determined by the equation

$$\frac{1}{\lambda^2(T,0)} = \frac{32\pi e^2}{\hbar^2 c^2} N(0) \xi_0^2 \Delta^2(T), \quad (22)$$

where $\Delta(T)$ is the equilibrium value of the energy gap, given by the equation

$$\Delta^2(T) = 9.38 k_B^2 T_{c0} (T_{c0} - T). \quad (23)$$

Now according to experiments,⁹⁻¹² in the small gap regions, BSCCO-2212 has a sizable superfluid density, whereas in the large-gap regions, the superfluid density is small or zero. If we interpret $1/\lambda^2(T,0)$ as proportional to the local superfluid density, then this experimental result implies that $1/\lambda^2(T,0)$ should vary *inversely* with $\Delta(T)$. In order for this to be consistent with Eq. (22), the quantity $N(0)\xi_0^2\Delta^2(T)$ should vary *inversely* with $\Delta(T)$. We therefore assume that $1/\lambda^2(T,0) \propto \Delta^{-x}(T)$, where $x > 0$ is some number which characterizes BSCCO-2212. While this is a highly oversimplified model, it does suggest how J_{IMD} is influenced by the inhomogeneity of the high- T_c layer.

III. MODEL CALCULATIONS

A. Analogy to a composite dielectric medium with a cubic nonlinearity

We now apply the above results to calculate J_{IMD} for several models of inhomogeneous superconducting layers. In

all cases, we attempt to choose the layer properties to resemble those reported in experiments on BSCCO-2212. Our goal is to solve Eq. (7) for $\mathbf{J}(\mathbf{x})$ and $\phi(\mathbf{x})$ for some prescribed inhomogeneous superconductor. We assume that $K_1(\mathbf{x})$ and $K_2(\mathbf{x})$ are specified, but random.

The present problem is *formally* equivalent to a randomly inhomogeneous dielectric with a cubic nonlinearity.^{16,17} In the latter problem, the electric field \mathbf{E} and electric displacement \mathbf{D} are related by

$$\begin{aligned} \mathbf{D}(\mathbf{x}) &= \epsilon(\mathbf{x})\mathbf{E}(\mathbf{x}) + \chi(\mathbf{x})|\mathbf{E}(\mathbf{x})|^2\mathbf{E}(\mathbf{x}), \\ \nabla \times \mathbf{E} &= 0, \end{aligned} \quad (24)$$

$$\nabla \cdot \mathbf{D} = 0.$$

For the intermodulation problem, the analogous equations are Eq. (7), supplemented by the steady-state charge conservation condition $\nabla \cdot \mathbf{J} = 0$. Thus, $-\nabla\phi$ plays the role of \mathbf{E} in the intermodulation problem and the phase ϕ plays the role of the scalar potential. The quantities $K_1(\mathbf{x})$ and $K_1(\mathbf{x})K_2(\mathbf{x})$ are analogous to the linear dielectric function $\epsilon(\mathbf{x})$ and cubic nonlinear susceptibility $\chi(\mathbf{x})$. The quantity $-\nabla\phi$ is, of course, curl-free like \mathbf{E} in an electrostatic problem. Thus, we are again connecting a divergence-free field to a curl-free field. To treat the intermodulation problem, therefore, we can use all the formal results previously derived for an inhomogeneous nonlinear dielectric, which we now briefly review.

For a material described by Eqs. (24), two useful coefficients are the *effective linear dielectric function* ϵ_e and the *effective cubic nonlinear susceptibility* χ_e . These quantities are defined in terms of the space-averaged electric field $\langle \mathbf{E} \rangle$ and displacement $\langle \mathbf{D} \rangle$ by

$$\langle \mathbf{D} \rangle = \epsilon_e \langle \mathbf{E} \rangle + \chi_e |\langle \mathbf{E} \rangle|^2 \langle \mathbf{E} \rangle. \quad (25)$$

As shown in Ref. 17, χ_e can be expressed as an average over the fourth power of the electric field in the associated *linear* composite. That is, if $\mathbf{E}_{\text{lin}}(\mathbf{x})$ is the electric field in a composite described by the linear relation $\mathbf{D}(\mathbf{x}) = \epsilon(\mathbf{x})\mathbf{E}(\mathbf{x})$, then χ_e is given by

$$\chi_e E_0^4 = \langle \chi(\mathbf{x}) |\mathbf{E}_{\text{lin}}(\mathbf{x})|^4 \rangle, \quad (26)$$

where E_0 is the applied electric field. If the composite medium has n components, the i th of which has nonlinear susceptibility χ_i , then Eq. (26) can be rewritten as

$$\chi_e = \sum_i p_i \chi_i e_i, \quad (27)$$

where p_i is the volume fraction of the i th component, e_i is an enhancement factor given by

$$e_i = \frac{\langle |\mathbf{E}(\mathbf{x})|^4 \rangle_{i,\text{lin}}}{E_0^4}, \quad (28)$$

and $\langle \cdots \rangle_{i,\text{lin}}$ means a space-average within the i th component in the related linear medium. Thus, e_i describes how much the fourth power of the electric field is enhanced in the i th component in the linear limit.

The moments e_i are difficult to compute exactly, except in a few very simple geometries. We have therefore chosen to make a decoupling approximation,^{18,19} specified by

$$\langle |\mathbf{E}(\mathbf{x})|^4 \rangle_{i,\text{lin}} \approx \langle |\mathbf{E}(\mathbf{x})|^2 \rangle_{i,\text{lin}}^2. \quad (29)$$

Clearly, the decoupling approximation (29) will be most accurate if the fluctuations $\langle |\mathbf{E}(\mathbf{x})|^4 \rangle_{i,\text{lin}} - \langle |\mathbf{E}(\mathbf{x})|^2 \rangle_{i,\text{lin}}^2$ within the i th component are small compared to $\langle |\mathbf{E}(\mathbf{x})|^4 \rangle_{i,\text{lin}}$ itself.¹⁹ This assumption is most likely to be accurate in geometries such that $|\mathbf{E}(\mathbf{x})|$ is uniform in each of the nonlinear components, but will be less accurate when the fluctuations are large. For example, in the so-called Hashin-Shtrikman geometry, in which one of the two components is embedded in the other, these fluctuations are small in the embedded component, and hence this approximation will be excellent if only the embedded component is nonlinear. However, in a composite near a percolation threshold, the fluctuations will be large and this approximation will be less accurate.

If we make the approximation (29), we can express $\langle |\mathbf{E}(\mathbf{x})|^2 \rangle_{i,\text{lin}}$ exactly in terms of the effective linear dielectric function ϵ_e through the relation

$$\frac{p_i \langle |\mathbf{E}(\mathbf{x})|^2 \rangle_{i,\text{lin}}}{E_0^2} = \frac{\partial \epsilon_e}{\partial \epsilon_i} \equiv F_i. \quad (30)$$

Here, $\partial \epsilon_e / \partial \epsilon_i$ is the partial derivative of ϵ_e with respect to ϵ_i , at constant ϵ_j ($j \neq i$) and constant volume fractions p_j . Given a simple analytical approximation for ϵ_e , these derivatives can be easily computed in closed form, thus yielding a simple analytical approximation for χ_e as

$$\chi_e = \sum_i \chi_i F_i^2 / p_i, \quad (31)$$

with $e_i = F_i^2 / p_i^2$. We will use this approach, combined with the analogy described above, to obtain approximations for the intermodulation coefficient in an inhomogeneous superconducting layer.

In the present work, we use two different approximation methods to calculate ϵ_e : the effective-medium approximation (EMA),^{20,21} and the Maxwell-Garnett approximation (MGA).²¹ The EMA is suitable for a binary composite with symmetrically distributed components, so that neither can be viewed as the inclusion or the host.¹⁸ In this case, if the components are isotropic, ϵ_e satisfies the quadratic equation

$$p_A \frac{\epsilon_A - \epsilon_e}{\epsilon_e + g(\epsilon_A - \epsilon_e)} + (1 - p_A) \frac{\epsilon_B - \epsilon_e}{\epsilon_e + g(\epsilon_B - \epsilon_e)} = 0. \quad (32)$$

Here p_A is the volume fraction of the component A , ϵ_A and ϵ_B are the dielectric functions of the components A and B , respectively, and g is a ‘‘depolarization factor.’’ $g=1/2$ in 2D and $g=1/3$ in three dimensions (3D). The physically meaningful solution of Eq. (32) is the root which varies continuously with p_A , approaches the correct limits at $p_A=0$ and 1, and has a nonnegative imaginary part when ϵ_A and ϵ_B are complex.¹⁸

The MGA is more suitable to a binary composite where one component can be regarded as a host in which the other

is embedded.¹⁹ When the host material is isotropic and linear, the effective dielectric function of the composite takes the form

$$\epsilon_e = \epsilon_h \left[1 + \frac{p_i(\epsilon_i - \epsilon_h)}{(1 - p_i)[\epsilon_h(1 - g) + \epsilon_i g] + p_i \epsilon_h} \right], \quad (33)$$

where p_i is the volume fraction of the inclusion, ϵ_i and ϵ_h are the dielectric functions of the inclusion and the host, respectively, and g is again the depolarization factor.

B. Application to an inhomogeneous superconductor

We can readily use the above analogy to compute the effective nonlinear coefficients for an inhomogeneous superconducting layer. We consider a superconducting layer comprised of two ‘‘components,’’ A and B , with areal fractions p_A and $p_B=1-p_A$, which have two different energy gaps. The two components are both intrinsic to the given sample, in the sense that they are not caused by the introduction of nonsuperconducting impurities. A realistic sample of BSCCO-2212 probably has a continuous distribution of gaps, but we make this simplification for computational convenience.

The effective cubic nonlinear coefficient $(K_1 K_2)_e$ takes the form

$$(K_1 K_2)_e = (K_1 K_2)_A p_A e_A + (K_1 K_2)_B p_B e_B. \quad (34)$$

J_{IMD} in Eq. (12) thus becomes

$$J_{\text{IMD}} = \frac{K_{1e}}{K_{2e}^{1/2}} = \frac{(K_1 K_2)_e}{K_{2e}^{3/2}}. \quad (35)$$

To apply the present formalism, we need to find suitable K_1 and K_2 values. From Eqs. (6) and (8), $K_1 = -(a/b) \times (\hbar e^* / m^*)$ and $K_1 K_2 = \hbar^3 e^* / (2m^{*2} b)$, giving $K_2 = -\hbar^2 / (2m^* a)$. Using $a = \alpha(t-1)$, where $t = T/T_{c0}$, and taking α and b from Eqs. (19) and (20), we find

$$K_1 = -\frac{a \hbar e^*}{b m^*} = \frac{\hbar c^2}{4\pi e^* \lambda^2(t, 0)} \quad (36)$$

and

$$K_2 = \frac{\hbar^2}{2m^* |a|} = \xi^2(t). \quad (37)$$

In typical cuprate superconductors, $\xi(t=0) \sim 15 \text{ \AA}$ and $\lambda(t=0, J=0) \sim 1500 \text{ \AA}$, so

$$K_2 = (15 \text{ \AA})^2. \quad (38)$$

To estimate the values of K_1 , we first assume that

$$\frac{1}{\lambda^2(T, 0)} \propto [\Delta(T)]^{-x}. \quad (39)$$

This assumption embodies the experimental observation that the superfluid density is relatively large in regions where the gap is relatively small. Thus, it is simply an effort to include relevant experimental features in the model, without attempting to explain them. In the model calculations below, we consider two different values of x , in order to see how this value affects the calculated J_{IMD} .

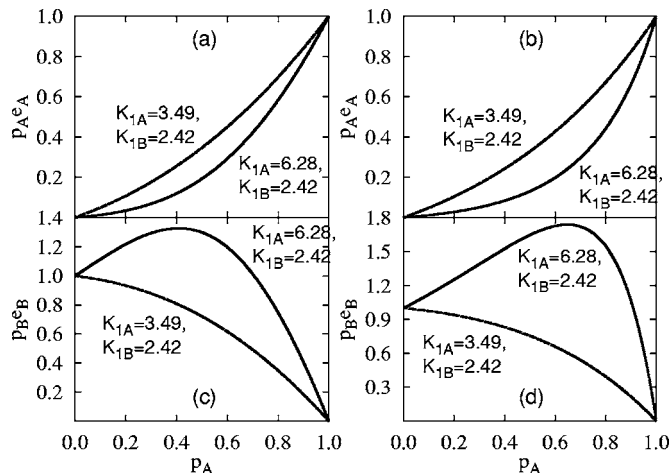


FIG. 1. Enhancement factors $p_A e_A$ and $p_B e_B$ for a 2D inhomogeneous superconductor consisting of a binary composite with two different energy gaps, which have the ratio K_{1A}/K_{1B} . The effective-medium approximation (EMA) is used in (a) and (c), while the Maxwell-Garnett approximation (MGA) is used in (b) and (d), assuming that A is surrounded by B . We use two different sets of K_1 's: $K_{1A}=6.28 \times 10^{11}$ esu/(cm s), $K_{1B}=2.42 \times 10^{11}$ esu/(cm s) and $K_{1A}=3.49 \times 10^{11}$ esu/(cm s), $K_{1B}=2.42 \times 10^{11}$ esu/(cm s) as indicated in the legend. In this and the following plots, the unit of K_{1A} and K_{1B} is 10^{11} esu/(cm s).

Equations (36) and (39) can be combined with experiment to get a rough estimate of K_1 . According to Ref. 9, $\Delta(T)$ ranges from 25 to 65 meV in optimally doped BSCCO-2212 at low T . We assume that the mean value, 45 meV, corresponds to $\lambda(0,0)=1500$ Å. This fixes the proportionality constant in Eq. (39). Using this proportionality constant and Eq. (36), we get

$$K_1 = 3.49 \times 10^{11} \left(\frac{\Delta(0)}{45 \text{ meV}} \right)^{-x} \frac{\text{esu}}{\text{cm s}}. \quad (40)$$

We first assume that $x=1$. Equation (40) implies that $\Delta(0)=25$ and 65 meV correspond, respectively, to $K_{1A}=6.28 \times 10^{11}$ esu/(cm s) and $K_{1B}=2.42 \times 10^{11}$ esu/(cm s). For K_{2A} and K_{2B} , we have no definite information from experiment. We therefore assume simply that $K_{2A}=K_{2B}$.

In Figs. 1 and 2, we show the calculated enhancement factors e_A and e_B and the corresponding intermodulation critical current density J_{IMD} for these models as functions of p_A . In Figs. 1(a), 1(c), and 2(a) we use the EMA [Eq. (32)], while in Figs. 1(b), 1(d), and 2(b) we use the MGA [Eq. (33)], with B considered as the host. In both cases, we combine these approximations with the decoupling approximation [Eqs. (29)–(31)] to obtain J_{IMD} .

Figure 2(a) shows that J_{IMD} increases linearly with p_A in the EMA. As in Eqs. (34) and (35), J_{IMD} has contributions from the nonlinearity of both components. While the enhancement factor e_A is never larger than unity, e_B can exceed unity, depending on the value of p_A . Thus, the nonlinearity of B has a larger influence on J_{IMD} than that of A . As a result, J_{IMD} behaves similarly to e_B , having a larger enhancement for the larger K_{1A}/K_{1B} . The MGA results differ little from the EMA results except for a broad peak around $p_A=0.9$ for the larger ratio of K_{1A}/K_{1B} . This peak results from the shift to higher values of p_A of both $p_B e_B$ and $p_A e_A$, seen in the MGA results of Fig. 1.

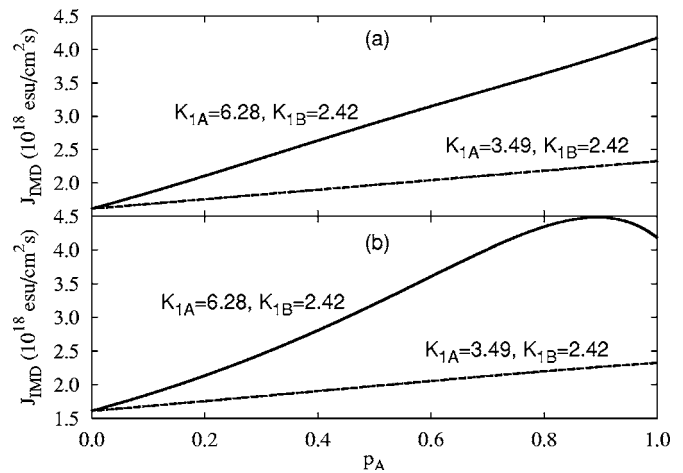


FIG. 2. Intermodulation critical supercurrent density J_{IMD} for the 2D inhomogeneous superconductor shown in Fig. 1. The EMA method is used in (a), while the MGA method is used in (b), assuming that A is surrounded by B . The two sets of K_1 's are the same as in Fig. 1. Note that 10^{18} power scale on the y axis.

We can also calculate the effective linear coefficients K_{1e} for these two models. In the 2D EMA, K_{1e} satisfies

$$p_A \frac{K_{1A} - K_{1e}}{K_{1A} + K_{1e}} + (1 - p_A) \frac{K_{1B} - K_{1e}}{K_{1B} + K_{1e}} = 0, \quad (41)$$

while in the 2D MGA with B considered as the host, we get

$$K_{1e} = K_{1B} \left[1 + \frac{2p_A(K_{1A} - K_{1B})}{(1 - p_A)(K_{1A} + K_{1B}) + 2p_A K_{1B}} \right]. \quad (42)$$

The K_{1e} 's are proportional to the effective superfluid densities (or the effective inverse-square penetration depths) of these 2D materials in the linear limit of very small applied currents. The values calculated from the EMA and MGA are shown in Figs. 3(a) and 3(b). Both increase monotonically with increasing areal fraction of the small-gap component A . The MGA results differ very little from the EMA results.

In Figs. 4–6, we show an analogous set of calculations, but with $x=3$. We again assume a binary distribution of gaps,

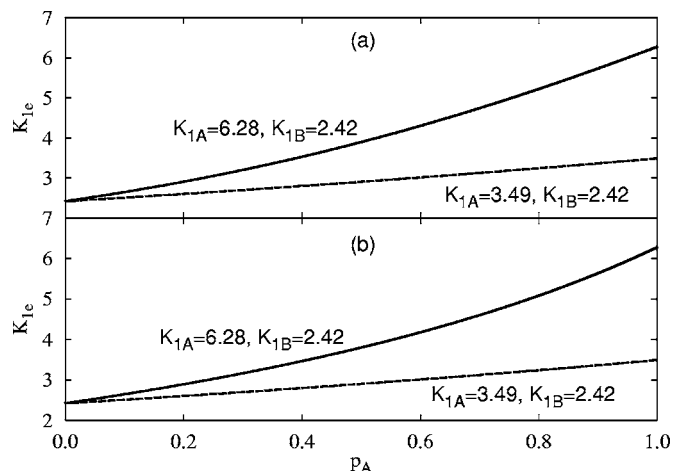


FIG. 3. Effective superfluid density K_{1e} for a 2D composite having the same values of K_{1A} and K_{1B} used in the calculations of Figs. 1 and 2. (a) EMA method and (b) MGA method, taking B (the component with the smaller superfluid density) as the host.

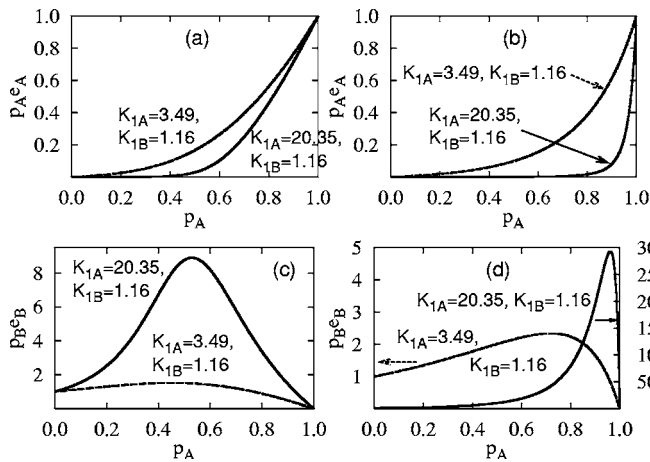


FIG. 4. Same as Fig. 1, except that $x=3$. The two sets of K_1 's are $K_{1A}=20.35 \times 10^{11}$ esu/(cm s), $K_{1B}=1.16 \times 10^{11}$ esu/(cm s) and $K_{1A}=3.49 \times 10^{11}$ esu/(cm s), $K_{1B}=1.16 \times 10^{11}$ esu/(cm s). The full curve is scaled to the right axis while the dashed line to the left in (d).

using the same gaps as in Figs. 1–3. Because of the larger x , the ratio K_{1A}/K_{1B} is larger than in Figs. 1–3. For $x=3$, using the same proportionality constant, we find that the gaps $\Delta(0)=65$ and 25 meV now correspond to $K_1=1.16 \times 10^{11}$ esu/(cm s) $\equiv K_{1B}$ and $K_1=20.35 \times 10^{11}$ esu/(cm s) $\equiv K_{1A}$.

For $x=3$, for the larger ratio of K_{1A}/K_{1B} , the enhancement factor $p_B e_B$ has clear peaks as a function of the areal fraction p_A . This behavior is shown in Figs. 4(c) and 4(d). The peak occurs at around the percolation threshold of $p_A=0.5$ in the EMA results, but at around $p_A=0.95$ in the MGA results. In addition, $p_B e_B$ is dramatically larger (~ 100) in the MGA than in the EMA, for the larger ratio of K_{1A}/K_{1B} . Note also that the EMA results are nearly symmetric about $p_A=0.5$ while the MGA results are very asymmetric. There is also a large difference between results for the two gap ratios in the MGA results, but a smaller one in the EMA. By contrast, $p_A e_A$ is monotonic in either the EMA or the MGA. Since J_{IMD} has two contributions, one from the enhancement of A and the other from the enhancement of B , one expects

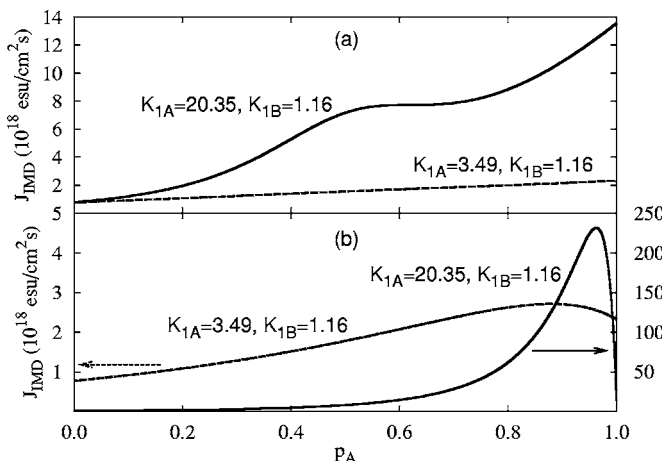


FIG. 5. Same as Fig. 2, except that $x=3$, so the two sets of K_1 's used are $K_{1A}=20.35 \times 10^{11}$ esu/(cm s), $K_{1B}=1.16 \times 10^{11}$ esu/(cm s) and $K_{1A}=3.49 \times 10^{11}$ esu/(cm s), $K_{1B}=1.16 \times 10^{11}$ esu/(cm s). The full curve is scaled to the right axis while the dashed line to the left in (b).

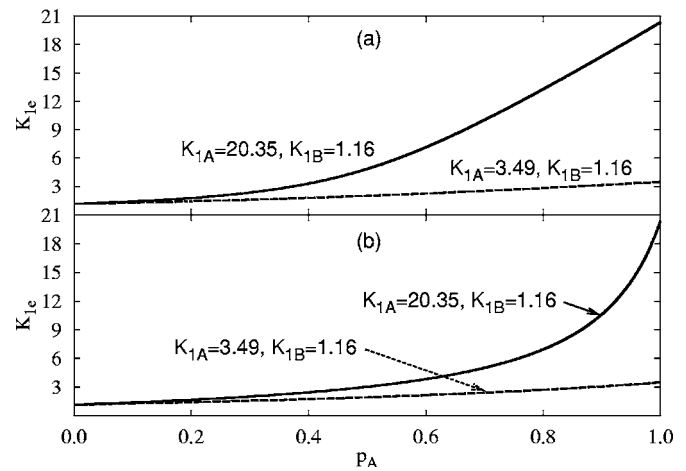


FIG. 6. Same as Fig. 3 except that $x=3$, corresponding to a much larger ratio of K_{1A}/K_{1B} .

that the behavior of J_{IMD} in the MGA results will mirror the enhancement factor $p_B e_B$ because $p_A e_A \ll p_B e_B$ for the larger ratio of K_{1A}/K_{1B} .

Figure 5 shows the behavior of J_{IMD} for the K_1 's shown in Fig. 4. As expected, and as already found for $x=1$, J_{IMD} for $x=3$ generally follows the trend of $p_B e_B$. In particular, because of the clear peak in $p_B e_B$, the EMA results show a weak broad peak near the percolation threshold p_c in J_{IMD} for the larger ratio of K_{1A}/K_{1B} . The EMA and MGA results differ greatly for the larger ratio of K_{1A}/K_{1B} , not only in the shape of the curves but also in the magnitude of J_{IMD} . In this case, the MGA results follow mostly the shape of the curve for $p_B e_B$. Although J_{IMD} increases monotonically with p_A in the EMA results, it drops sharply above $p_A=0.95$ for the larger ratio of K_{1A}/K_{1B} in the MGA results. Overall, the $x=3$ case produces a much larger value of J_{IMD} for the larger ratio of K_{1A}/K_{1B} . Thus, for a device requiring a large J_{IMD} , these results suggest that the best results would be obtained using an inhomogeneous superconductor with a large gap difference and a large x in a Maxwell-Garnett geometry.

Figure 6 shows the effective superfluid densities K_{1e} with $x=3$. For the smaller ratio of K_{1A}/K_{1B} , the EMA results differ little from the MGA results as we found previously in Fig. 3. However, for the larger ratio of K_{1A}/K_{1B} , the two differ significantly.

There is no distinction between the inclusion and the host in the EMA method, but there is in the MGA method. In our MGA results thus far, we have assumed that A (the component with the smaller gap) is the inclusion and that B is the host. We now consider the reverse configuration, where B is surrounded by A . Results for this configuration are shown in Figs. 7–9. The MGA results with $x=1$ shown in Figs. 7(a), 7(b), 8(a), and 9(a) are very similar to the EMA results in Figs. 1(a), 1(c), 2(a), and 3(a), respectively; indeed, the results for J_{IMD} and K_{1e} are almost identical in the two approximations. For the larger value of K_{1A}/K_{1B} , the enhancement factor $p_B e_B$ is smaller in Fig. 7(b) than in Fig. 1(c). In general, the results for this version of MGA do not show the dramatically large increases in J_{IMD} seen in Fig. 5 for the larger ratio of K_{1A}/K_{1B} . In Figs. 7(c), 7(d), 8(b), and 9(b) we show the same MGA calculations for $p_A e_A$, $p_B e_B$, J_{IMD} , and

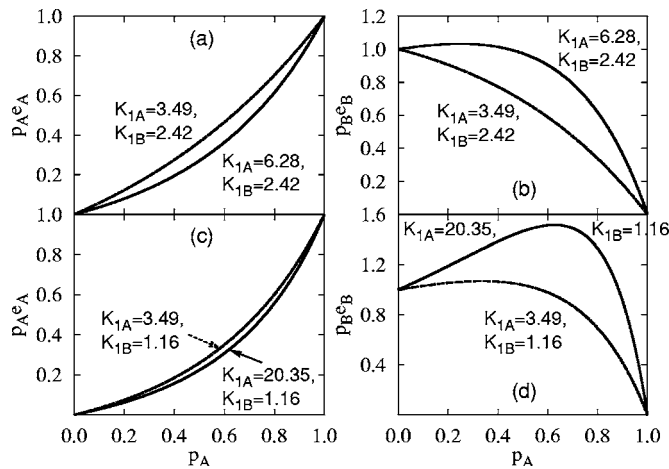


FIG. 7. Same as Fig. 1, except that the MGA method is used in all cases, assuming that B is surrounded by A . The two sets of K_1 's are $K_{1A}=6.28 \times 10^{11}$ esu/(cm s), $K_{1B}=2.42 \times 10^{11}$ esu/(cm s) and $K_{1A}=3.49 \times 10^{11}$ esu/(cm s), $K_{1B}=2.42 \times 10^{11}$ esu/(cm s) in (a) and (b), while they are $K_{1A}=20.35 \times 10^{11}$ esu/(cm s), $K_{1B}=1.16 \times 10^{11}$ esu/(cm s) and $K_{1A}=3.49 \times 10^{11}$ esu/(cm s), $K_{1B}=1.16 \times 10^{11}$ esu/(cm s) in (c) and (d).

K_{1e} but with $x=3$. The behavior does not differ greatly from that seen in the cases with $x=1$, except for an increase in the magnitudes of J_{IMD} and K_{1e} for the larger ratio of K_{1A}/K_{1B} . By contrast, the MGA results for a B host show some dramatic peaks for the larger ratio of K_{1A}/K_{1B} , as shown earlier.

IV. DISCUSSION

In this paper, we have calculated the intermodulation critical current J_{IMD} in an inhomogeneous 2D superconductor characterized by a binary distribution of energy gaps. To carry out this calculation, we used an analogy between the effective cubic nonlinear response of an inhomogeneous superconductor and the effective cubic nonlinear susceptibility of a composite dielectric medium. Using this analogy, we can apply the formalism previously developed to treat the nonlinear dielectric composite to the inhomogeneous superconductor. We found that the cubic nonlinear response of the

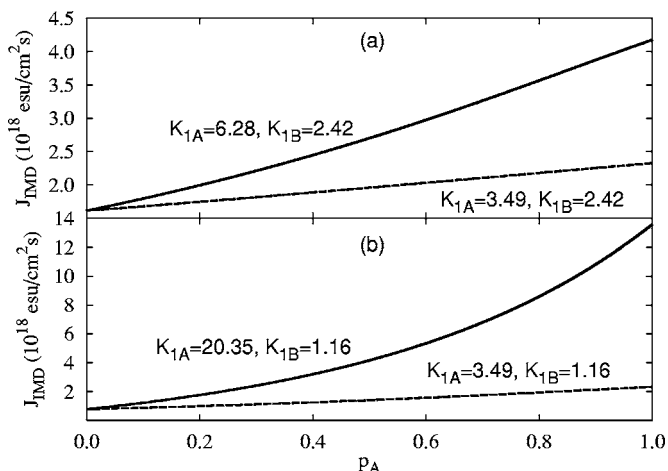


FIG. 8. Intermodulation critical supercurrent density J_{IMD} for the 2D inhomogeneous superconductor shown in Fig. 7. The MGA method is used in (a) and (b), assuming that B is surrounded by A . The two sets of K_1 's used are the same as in Fig. 7. Note that 10^{18} power scale on the y axis.

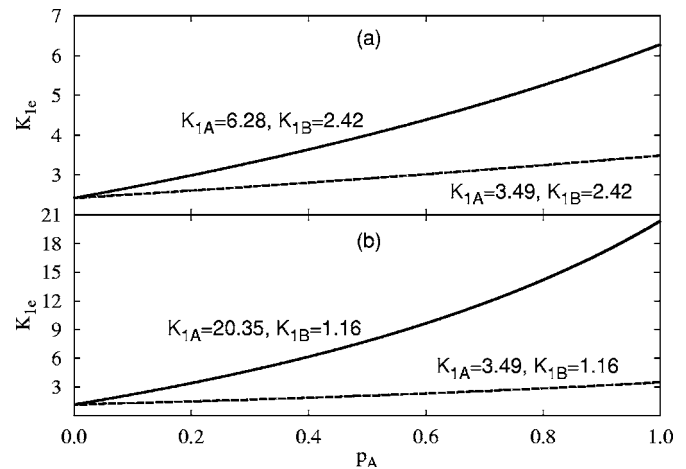


FIG. 9. Effective superfluid density K_{1e} corresponding to Figs. 7 and 8.

superconductor could be expressed in terms of the cubic response of each “component” (i.e., energy gap) and two enhancement factors, each describing the field and current distributions in the related *linear* medium.

In order to simplify our calculations, we have assumed that the superconducting layer has a binary distribution of energy gaps, Δ_A and Δ_B (with $\Delta_B > \Delta_A$), and we have considered three plausible topologies: “effective-medium” topology (A and B symmetrically distributed) and two “Maxwell-Garnett” topologies (A embedded in B and B embedded in A). We have treated all three using a simple nonlinear decoupling approximation.

The results for J_{IMD} are dramatically dependent on the assumed topologies. The EMA and the MGA with B in A give rather similar results for ratios of Δ_B/Δ_A close to unity, and only modest enhancements of J_{IMD} at any concentrations of A . However, the MGA with A (the component with the smaller gap) embedded in B leads to huge enhancements in J_{IMD} compared to its value in either pure A or pure B , provided that the two gap values are sufficiently different and that x is large.

In view of these differences, it is of interest to compare our results with the detailed measurements of Lang *et al.*¹² These experiments do not provide results directly for J_{IMD} . However, they do provide some hints about a possible connection. In particular, in experiments on as-grown Ni-doped samples, Ni scattering resonances were observed only in the regions where $\Delta < 50$ meV, which were identified as superconducting regions, i.e., regions with superconducting phase coherence. In our results, most of the enhancement in J_{IMD} comes from K_A , which corresponds to the component with a low energy gap. Therefore the regions of enhanced J_{IMD} correspond to regions of small energy gap, and also regions of enhanced phase coherence according to the measurements of Ref. 12.

A striking feature of our results is the large difference between the EMA results and the MGA results, especially for binary composites with a large x and very different energy gaps. Which of these approximations is the most correct? In fact, there is no single correct answer for all materials: the correct choice depends on the actual topology of the material of interest. In particular, we do not know, beforehand,

whether the energy gaps in an inhomogeneous superconductor are distributed at random throughout the CuO_2 planes or whether regions with one magnitude of energy gap are preferentially surrounded by those of the other energy gap. This topology determines whether we should use the EMA or the MGA approach.

In the experimental gap maps,¹² the low- Δ regions are surrounded by the high- Δ regions in the underdoped BSCCO-2212 sample, but the high- Δ regions are surrounded by the low- Δ regions in the slightly overdoped as-grown BSCCO-2212 sample. Therefore, it appears that we can apply the MGA method to both cases, but with the roles of inclusion and host reversed in each case. But even this description of the distribution may be a simplification of the true gap distribution, which is probably continuous, not a discrete binary distribution. Ideally, we should consider such a continuous distribution of energy gaps.

The great sensitivity of J_{IMD} to composite geometry, as found in the present work, is not surprising, in view of earlier work on transport in linear and nonlinear composite conductors and dielectric media. For example, it is well known that the critical exponents describing transport, especially nonlinear transport, in composite media are sensitive to features of the local geometry.^{22–25} We speculate that, depending on the precise nature of this geometry, J_{IMD} either diverges or goes to zero near a percolation threshold according to an appropriate critical exponent.

In summary, we have presented a general formalism for calculating the intermodulation coefficient and the corresponding intermodulation supercurrent density J_{IMD} of an inhomogeneous superconductor. We have also given a simple way to calculate J_{IMD} approximately in several geometries. Since such inhomogeneities are known to exist in many of the high- T_c cuprate superconductors, this formalism is directly relevant for treating an important property of these materials. We find that the resulting J_{IMD} is very sensitive to the exact spatial distribution of gaps within the inhomogeneous layer and thus may increase or decrease, depending on the topology. Our calculations show that one way to achieve a large J_{IMD} is to have the component with the smaller gap and larger superfluid density embedded in the component with the opposite properties. This appears to be the topology seen in the underdoped BSCCO-2212, which thus may be well suited for a material with a large J_{IMD} .

Finally, we comment briefly on possible device implications of the present results. A useful microstrip resonator would usually have a minimum of intermodulation, i.e., interference between different frequencies.²⁶ To achieve this,

one would probably want a J_{IMD} which is as large as possible, because this would lead to $1/\lambda^2(T, J)$ which has the weakest dependence on current. Surprisingly, we find here that J_{IMD} can actually be *increased* in some inhomogeneous superconductors, provided that the topology is suitable. Thus the inhomogeneity which appears to be unavoidable in the high- T_c cuprates may even be an advantage in constructing useful microwave devices.

ACKNOWLEDGMENTS

This work was supported by NSF Grant DMR04-13395. We are grateful to D. J. Bergman for helpful discussions. Some of the calculations were carried out on the P4 Cluster at the Ohio Supercomputer Center, with the help of a grant of time.

- ¹J. G. Bednorz and K. A. Müller, Z. Phys. B: Condens. Matter **64**, 189 (1986).
- ²Balam A. Willemsen, T. Dahm, and D. J. Scalapino, Appl. Phys. Lett. **71**, 3898 (1997).
- ³T. Dahm and D. J. Scalapino, Appl. Phys. Lett. **69**, 4248 (1996).
- ⁴T. Dahm and D. J. Scalapino, J. Appl. Phys. **81**, 2002 (1997).
- ⁵S. K. Yip and J. A. Sauls, Phys. Rev. Lett. **69**, 2264 (1992).
- ⁶D. Xu, S. K. Yip, and J. A. Sauls, Phys. Rev. B **51**, 16233 (1995).
- ⁷B. P. Stojković and O. T. Valls, Phys. Rev. B **51**, 6049 (1995).
- ⁸J. McDonald, J. R. Clem, and D. E. Oates, Phys. Rev. B **55**, 11823 (1997).
- ⁹S. H. Pan *et al.*, Nature (London) **413**, 282 (2001).
- ¹⁰A. C. Fang, L. Capriotti, D. J. Scalapino, S. A. Kivelson, N. Kaneko, M. Greven, and A. Kapitulnik, Phys. Rev. Lett. **96**, 017007 (2006).
- ¹¹C. Howald, P. Fournier, and A. Kapitulnik, Phys. Rev. B **64**, 100504(R) (2001).
- ¹²K. M. Lang, V. Madhavan, J. E. Hoffman, E. W. Hudson, H. Eisaki, S. Uchida, and J. C. Davis, Nature (London) **415**, 412 (2002).
- ¹³R. Jamei, J. Robertson, E.-A. Kim, A. Fang, A. Kapitulnik, and S. A. Kivelson, e-print cond-mat/0608318.
- ¹⁴We do not, in this paper, consider the dependence of the coefficient J_{IMD} on the angle θ between the current and the a axis of the CuO_2 plane, such as would be expected in a superconductor having a $d_{x^2-y^2}$ order parameter.
- ¹⁵P. G. de Gennes, *Superconductivity of Metals and Alloys* (Benjamin, New York, 1966), pp. 173–180.
- ¹⁶X. Zhang and D. Stroud, Phys. Rev. B **49**, 944 (1994).
- ¹⁷D. Stroud and P. M. Hui, Phys. Rev. B **37**, 8719 (1988).
- ¹⁸D. Stroud and Van E. Wood, J. Opt. Soc. Am. B **6**, 778 (1989).
- ¹⁹X. C. Zeng, D. J. Bergman, P. M. Hui, and D. Stroud, Phys. Rev. B **38**, 10970 (1988).
- ²⁰D. A. G. Bruggeman, Ann. Phys. **24**, 636 (1935).
- ²¹For reviews, see, e.g., R. Landauer, AIP Conf. Proc. **40**, 2 (1978); D. J. Bergman and D. Stroud, Solid State Phys. **46**, 147 (1992).
- ²²R. Rammal, C. Tannous, P. Breton, and A.-M. S. Tremblay, Phys. Rev. Lett. **54**, 1718 (1985).
- ²³B. I. Halperin, S. Feng, and P. N. Sen, Phys. Rev. Lett. **54**, 2391 (1985).
- ²⁴R. Rammal, Phys. Rev. Lett. **55**, 1428 (1985).
- ²⁵A.-M. S. Tremblay, S. Feng, and P. Breton, Phys. Rev. B **33**, 2077 (1986).
- ²⁶See, e.g., S. K. Remillard, H. R. Yi, and A. Abdelmonem, IEEE Trans. Appl. Supercond. **13**, 3797 (2003).